Bull. Mater. Sci., Vol. 40, No. 6, October 2017, pp. 1241–1245
DOI 10.1007/s12034-017-1481-2

Melt-assisted synthesis to lanthanum hexaboride nanoparticles and cubes

CHUN-LIANG HANG, LI-XIA YANG*, FENG WANG, YAN-BIN XU and CHEN-YU YI
School of Chemistry and Materials Science, Ludong University, Yantai 264025, People's Republic of China
*Author for correspondence (yanglx2003@163.com)

MS received 24 June 2016; accepted 21 February 2017; published online 22 September 2017

Abstract. Lanthanum hexaboride (LaB_6) nanocrystals and cubes were successfully synthesized at 700°C for 2 h under argon atmosphere by a melt-assisted method using $LaCl_3$ and $NaBH_4$ as reactants, NaCl–KCl or zinc or NaCl–KCl–zinc as reaction melt. The obtained products were characterized by X-ray diffraction (XRD), scanning electron microscopy (SEM), transmission electron microscopy (TEM) and Raman spectroscopy. XRD patterns and Raman spectra confirmed the formation of LaB_6 with high purity. TEM and SEM results showed LaB_6 powders prepared in mixed molten salts of NaCl–KCl were mainly composed of nanoparticles with sizes of ca. 8 nm. The morphology of LaB_6 presented as regular cubes (100–300 nm) when metal zinc was used as reaction melt. Photothermal conversion test indicated that nanoparticles had a better photothermal conversion performance than cubes.

Keywords. LaB_6; microstructure; melt-assisted synthesis; photothermal conversion.

1. Introduction

Lanthanum hexaboride (LaB_6) has a simple cubic structure of CsCl type (space group, Pm-3m) with B_6 octahedra occupying the corners of the cube and La atoms in the centre [1–3]. Boron atoms are connected by covalent bonds, and lanthanum atoms and boron atoms are linked by ionic bonds [3]. Because of unique chemical bonds and crystal structure, LaB_6 was provided with excellent chemical and physical properties such as high melting temperature [4], thermal stability [5,6], chemical stability [7], low work function [8,9], scattering and absorption function [10,11], and photothermal conversion properties [12]. LaB_6 has been found in the applications of a large variety of devices requiring electron emission because of its low work function (2.5–2.6 eV) [5,8], such as transmission electron microscope (TEM) and scanning electron microscope (SEM). Many researchers began to study the optical properties of LaB_6. Schelm and Smith [13] put LaB_6 powder into the poval and obtained composites which had better heat insulation behaviour when the mean particle size was <80 nm. Yifei Yuan *et al* [14] studied the size effect of LaB_6 particles on optical properties of LaB_6/polymer composites and found that particles with size of ∼70 nm showed the best optical properties. In addition, LaB_6 nanoparticles could be used as near-infrared (NIR) photothermal conversion material in biomedical applications as drug carrier. Lai and Chen [15] reported LaB_6@C–SiO_2 core–shell structure which exhibited an excellent NIR photothermal conversion property, suggesting that LaB_6 has no significant cytotoxicity.

To date, a good number of synthesis routes have been explored to prepare LaB_6, such as pure elemental synthesis [16], carbothermal method [17], borothermic reduction method [18], self-propagating synthesis [19], high-temperature and high-pressure synthesis [20], chemical vapour deposition method [21], zone melting method [22] and melt-flux method [23,24]. Recently, $NaBH_4$ was proved to be a good boron source for the synthesis of borides. Yifei Yuan *et al* [25] reported a route to prepare LaB_6 nanoparticles through a solid-state reaction of $LaCl_3$ with $NaBH_4$ at 1200°C under vacuum condition. However, boron volatilized immensely in such a vacuum solid state reaction. Maofeng Zhang *et al* [26] reported a route to synthesize LaB_6 nanocrystalline at 400 °C through a solid-state reaction of metallic magnesium powder with $NaBH_4$ and $LaCl_3$. Although LaB_6 can be prepared by low-temperature solid state reaction in an autoclave, it made higher demand to reaction vessels.

In this paper, we reported a new route i.e., melt-assisted method to prepare LaB_6 nanoparticles and cubes at 700°C through a reaction of $NaBH_4$ and $LaCl_3$ in molten solution under the protection of argon. Two types of molten solutions including NaCl–KCl mixed solution and zinc melt were used. This simple method can achieve the preparation of LaB_6 powders at relatively low reaction temperature. Finally, photothermal conversion properties of LaB_6 powders were measured.

2. Experimental

2.1 *Materials*

Lanthanum chloride hydrate ($LaCl_3 \cdot nH_2O$, AR), zinc powder (Zn, AR), potassium chloride (KCl, AR), sodium chloride (NaCl, AR) and sodium borohydride ($NaBH_4$, 96%) were purchased from Sinopharm Chemical Reagent Co. Ltd (Shanghai, China). Hydrochloric acid (HCl, AR) was purchased from Laiyang Economic and Technological Development Zone Refined Chemical Plant (Laiyang, China).

2.2 *Sample preparation*

In a typical procedure, 0.5570 g $LaCl_3 \cdot nH_2O$, 0.5155 g $NaBH_4$, 0.5000 g NaCl and 0.5000 g KCl were hand-grinded for half an hour under an infrared lamp and transferred to a porcelain crucible of 25 ml capacity. The crucible was put into the tube furnace under argon atmosphere with a flow of 200 ml min^{-1}. The furnace was heated and soaked at 700°C for 2 h. Then, the crucible was taken out at room temperature and the product was washed with dilute HCl and deionized water to remove NaCl, KCl and other impurities. The final products were vacuum-dried at 60°C. Black powder was obtained and marked as sample 1.

For the preparation of sample 2, all experimental parameters were consistent with sample 1 except that NaCl and KCl were used instead of 1.0615 g zinc powder. Sample 3 was prepared by adding of 1.0615 g zinc powder on the basis of sample 1 and the other experimental parameters were same as sample 1.

2.3 *Sample characterization*

X-ray diffraction (XRD) patterns were collected using a Rigaku D/max 2500 VPC X-ray diffractometer with a CuKα X-ray to identify the crystal structure and phase. SEM images were taken on a FEI-Sirion 200 (Philips, Holland). TEM images, SAED patterns and HRTEM images of the samples were observed with a TEM (JEM2100F, Japan). Raman spectra were measured on Laser Confocal Micro-Raman Spectroscopy (LabRAM HR800, Horiba Jobin Yvon) with 532 nm laser as an excitation light source. With the increase in temperature of LaB_6 solution, 808 nm NIR laser was delivered through a 4 ml quartz cuvette with 1 ml of dispersion with different concentrations and a power density of 2.0 W cm^{-2}. NIR laser was 6 cm away from quartz cuvette. A thermocouple with an accuracy of ±0.1 was inserted into the dispersion perpendicular to the laser path. The temperature was recorded per 20 s for 5 min.

3. Results and discussion

XRD patterns were employed to confirm the crystallinity and purity of LaB_6. Figure 1 gives XRD patterns of samples 1, 2 and 3. All diffraction peaks of three samples can be easily indexed as cubic crystal system (space group: pm-3m (221)) of single-phase LaB_6 with no other impurities. It can be noted that XRD peaks of sample 1 were widely broadened when compared with those of sample 2, showing that particles prepared in mixed salt of NaCl–KCl were smaller than those synthesized in zinc melt. All the three XRD patterns show well-defined peaks which indicated the crystallinity of the products. The calculated lattice constant $a = 4.154$ Å (sample 1); 4.166 Å (sample 2); 4.154 Å (sample 3), is very close to the reported data (JCPDS card no: 65-1831), indicating that LaB_6 can be successfully prepared through such a melt-assisted method.

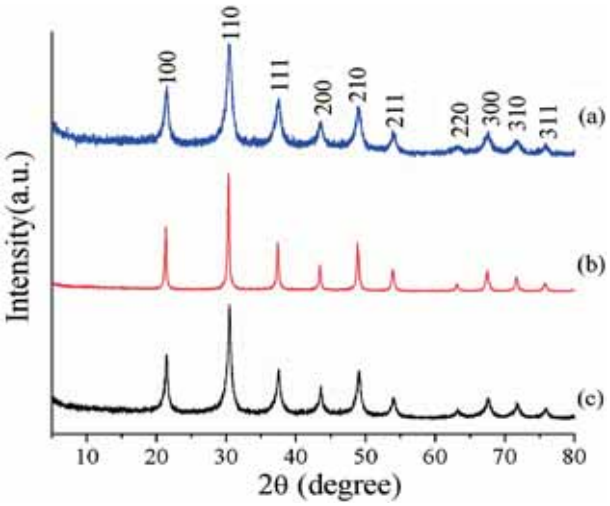

Figure 1. XRD patterns of samples. (**a**) sample 1; (**b**) sample 2 and (**c**) sample 3.

The morphologies of as-prepared LaB_6 were examined by SEM as shown in figure 2. Figure 2a indicates that sample 1 consists of nanoparticles with mean grain size of ∼30 nm. The particles were vigorously agglomerated, some of them were sintered together. Figure 2b shows the image of sample 2, the particles mainly show cubic morphology with size distribution ranging from 200 to 300 nm. Nanoparticles easily formed in mixed molten of NaCl–KCl, while LaB_6 cubes can be obtained in zinc melt, morphologies of LaB_6 prepared in NaCl–KCl–zinc were shown in figure 2c. It was found that sample 3 was composed of irregularly shaped chunk with diameters of 100–300 nm, and on the surface, there are some nanoparticles with size of ∼40 nm. The morphology of sample 3 is an intermediate structure between samples 1 and 2. LaB_6 cubes easily formed in zinc melt mainly because the melting point of zinc was lower than that of NaCl–KCl. Under the same experimental condition, chemical reaction occurred earlier in zinc melt, the size of crystal could grow larger until the size reaches a critical size to form cubes with the lowest surface free energy. In addition, the preferred growth of crystal surfaces is another reason [23]. From the above results, it can be seen that the choice of melt made it easier to control the morphology of LaB_6 powder.

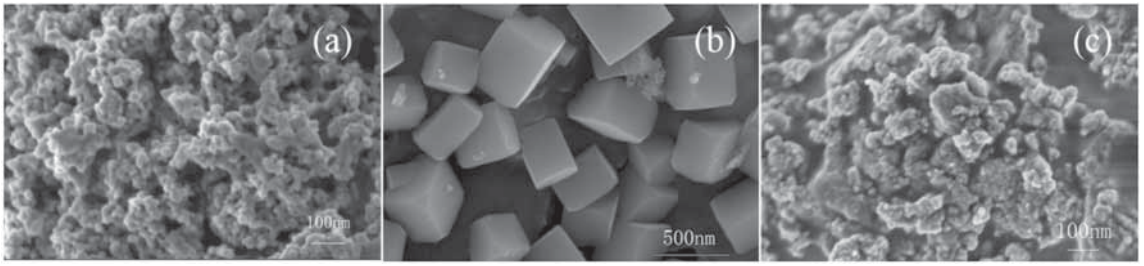

Figure 2. SEM images of samples. (**a**) Sample 1; (**b**) sample 2 and (**c**) sample 3.

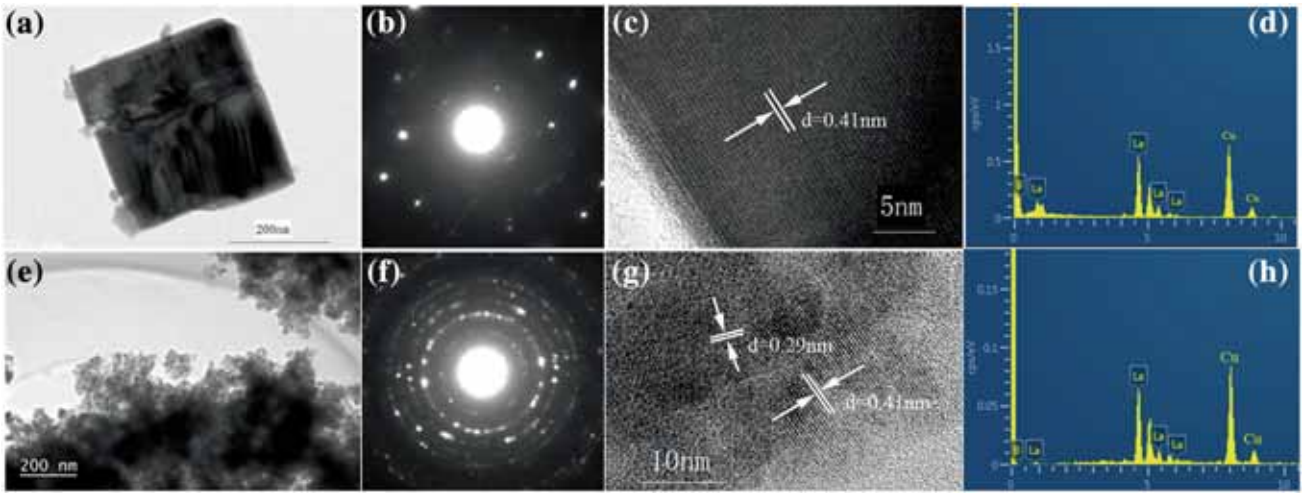

Figure 3. TEM image, SAED pattern, HRTEM image and EDS spectrum of (**a–d**) sample 2; (**e–h**) sample 1.

Further, characterization was performed by means of TEM to explore the microstructure. Figure 3a–d shows the TEM images and EDS spectrum of LaB_6 cubes (sample 2) prepared in zinc melt. As can be seen from figure 3a, LaB_6 cubes with particles size of ∼300 nm were prepared. Figure 3c shows a typical HRTEM image of LaB_6 cubes, the lattice spacing of 0.41 nm matches well with the standard JCPDS card value. SAED pattern of LaB_6 cube indicates that the cube was monocrystalline. Figure 3e–h shows TEM images and EDS spectrum of LaB_6 nanoparticles prepared in NaCl–KCl mixed salt. SAED pattern of LaB_6 nanoparticles indicates its polycrystalline nature. The nanoparticles consist of small single crystals with main grain sizes of ∼8 nm. Lattice spacings of 0.41 and 0.29 nm correspond to (100) and (110) crystal planes of LaB_6, respectively. Figure 3d and h shows the EDS spectra of the obtained LaB_6 samples. The results showed that both LaB_6 cubes and nanoparticles contained La and B, and no contamination element was detected (copper was detected owing to the copper grid), which further confirmed the successful synthesis of single phase LaB_6 using such a melt-assisted method.

Figure 4 shows the Raman spectra of LaB_6 nanoparticles and cubes. Three strong peaks of both samples 1 and 2 were observed around 721(T_{2g}), 1101(E_g) and 1235(A_{1g}) cm^{-1}. All these peaks were in agreement with the earlier reports

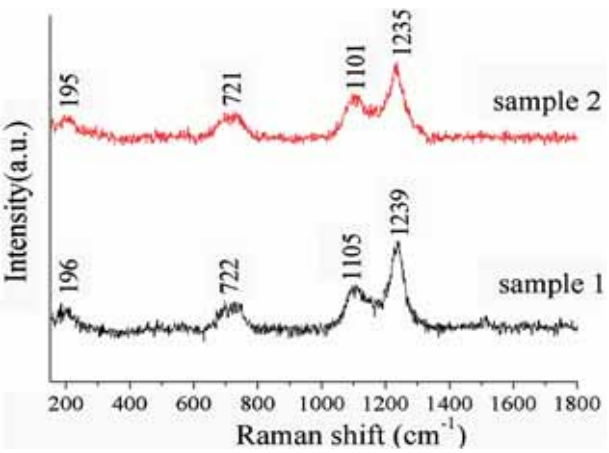

Figure 4. Raman spectra of LaB_6 samples.

[27,28]. In addition, another characteristic band of LaB_6 at 196 cm^{-1} was reported in the literature [8]. Raman spectra of both samples 1 and 2 indicated the formation of LaB_6.

Figure 5 shows the variations of solution temperature with irradiation time for water and LaB_6 aqueous solution under NIR laser irradiation with different LaB_6 concentrations. It was found that under the irradiation of light with a

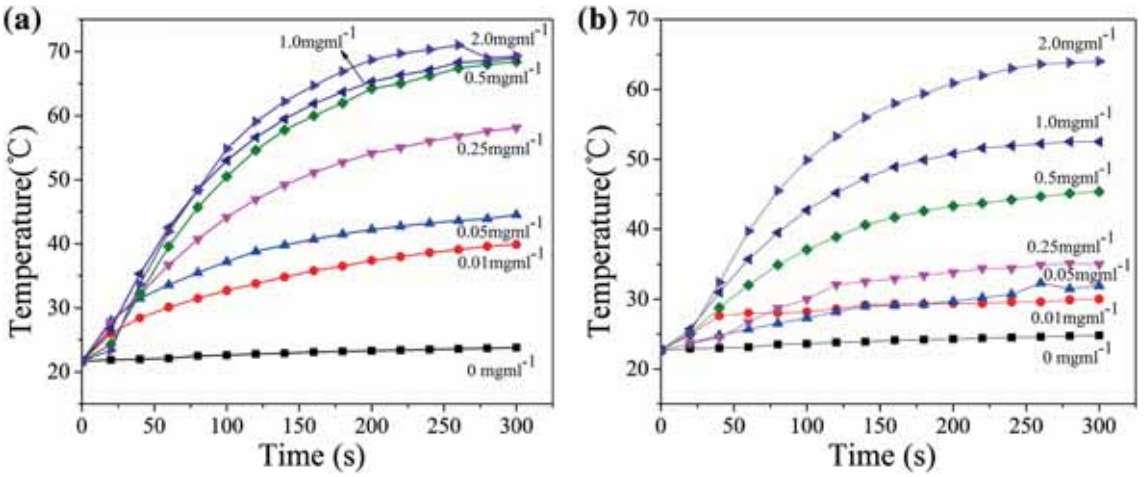

Figure 5. Photothermal heating curves of samples with different concentrations. (**a**) Sample 1 and (**b**) sample 2.

wavelength of 808 nm for 5 min, water temperature raised slightly from 21.7 to 23.8 °C. With the addition of LaB_6 nanopartilces and cubes, the temperature of LaB_6 aqueous solution can be greatly improved. Also, temperature increase became more significant with increase in the concentration of both LaB_6 nanopartilces and cubes. In our experiments, when the concentration of LaB_6 aqueous solution reached 2.0 mg ml^{-1}, the highest temperature can be obtained. For LaB_6 nanopartilces (figure 5a), the temperature reached 71°C at about 250 s. Figure 5b shows the temperature rise curves of LaB_6 cubes. The highest temperature was 64°C after light irradiation for 300 s, which was lower than that of LaB_6 nanoparticles. Because of small sizes, nanoparticles had larger specific surface than cubes and contacted with light fully and conducive to the generation of plasma resonance effect. In addition, cubes with large sizes will reduce the transmittance of light to solution, which caused poor photothermal conversion performance than nanoparticles.

4. Conclusions

In summary, LaB_6 nanoparticles and cubes have been successfully synthesized by a melt-assisted method at 700°C in a tube furnace starting from $LaCl_3 \cdot nH_2O$ and $NaBH_4$ under the protection of argon atmosphere. XRD patterns and Raman spectra confirm the crystallization and the formation of LaB_6. TEM and SEM images clearly show the morphologies of LaB_6. In the mixed salts of NaCl–KCl, LaB_6 nanoparticles were prepared with smaller sizes. In pure zinc melt, it is easy to form LaB_6 cubes with regular shape. Photothermal conversion experiments indicated that nanoparticles had a better photothermal conversion performance than cubes. Compared with previous routes, the present route has advantages of simplicity, low-temperature, low requirement on equipment and more economical. This method opens a new way to synthesis of other rare-earth metal hexaborides at lower temperature.

Acknowledgements

We are grateful for the financial support by National Natural Science Foundation of China (No. 51102128), Shandong Province Natural Science Foundation (ZR2011EL005) and the Youth Science Foundation of Shandong Province (BS2012CL011).

References

[1] Igityan A, Kafadaryan Y, Aghamalyan N, Petrosyan S, Badalyan G, Hovsepyan R *et al* 2014 *Thin Solid Films* **564** 415
[2] Trenary M 2012 *Sci. Technol. Adv. Mater.* **13** 1
[3] Johnson R W and Daane A H 1961 *J. Phys. Chem.* **65** 909
[4] Kakiage M, Shiomi S, Yanase I and Kobayashi H 2015 *J. Am. Ceram. Soc.* **98** 2724
[5] Sonber J K, Sairam K, Murthy T and Hubli R C 2014 *J. Eur. Ceram. Soc.* **34** 1155
[6] Wang D, Zhang L, Min G H, Yu H S and Yuan Y F 2011 *Appl. Surf. Sci.* **257** 6418
[7] Wang L, Xu L, Ju Z and Qian Y T 2010 *Cryst. Eng. Commun.* **12** 3923
[8] Bao L H, Wuren T Y, Wei W and Tegus O 2014 *Mater. Charact.* **97** 69
[9] Patra R, Ghosh S and Ganguli A K 2012 *RSC Adv.* **2** 7875
[10] Schelm S, Smith G B, Garrett P D and Fisher W K 2005 *J. Appl. Phys.* **97** 124314
[11] Hong Y, Zhang X S, Li B, Li M Z, Shi Q L, Wang Y Y *et al* 2013 *J. Rare Earth* **31** 1096
[12] Chen C J and Chen D H 2012 *Chem. Eng. J.* **180** 337
[13] Schelm S and Smith G B 2003 *Appl. Phys. Lett.* **82** 4346
[14] Yuan Y F, Zhang L, Hu L J, Wang W and Min G H 2011 *J. Solid State Chem.* **184** 3364

[15] Lai B H and Chen D H 2013 *Acta Biomater.* **9** 7556
[16] Lafferty J M 1951 *J. Appl. Phys.* **22** 299
[17] Hasan M, Sugo H and Kisi E 2013 *J. Alloys Compd.* **578** 176
[18] Hiebl K and Sienko M J 1980 *Inorg. Chem.* **19** 2179
[19] Jiang N, Wang W M, Fu Z Y, Wang H, Wang Y C and Zhang J Y 2010 *Adv. Mater. Res.* **105–106** 351
[20] Wu W Y, Xu J Y, Peng K W and Tu G F 2007 *J. Rare Earth* **25** 282
[21] Han Z, Qi Z, Tang J and Qin L 2005 *J. Am. Chem. Soc.* **127** 2862
[22] Otani S, Tanaka T and Ishizawa Y 1990 *J. Cryst. Growth* **100** 658
[23] Li P T, Li C, Nie J F, Qu Y J and Liu X F 2012 *Cryst. Eng. Commun.* **15** 411
[24] Olsen G H and Cafiero A V 1978 *J. Cryst. Growth* **44** 287
[25] Yuan Y F, Zhang l, Liang L M, He K, Liu R and Min G H 2011 *Ceram. Int.* **37** 2891
[26] Zhang M F, Yuan L, Wang X Q, Fan H, Wang X Y, Wu X Y *et al* 2008 *J. Solid State Chem.* **39** 294
[27] Teredesai P, Muthu D V S, Chandrabhas N, Meenakshi S, Vijayakumar V, Modak P *et al* 2004 *Solid State Commun.* **129** 791
[28] Yahia Z, Turrell S, Mercurio J P and Turrell G 1993 *J. Raman Spectrosc.* **24** 207